PREDICTIVE CONTROL APPLIED IN 3-PHASE SQUIRREL CAGE INDUCTION MOTOR FOR ZERO SPEED

Lucas R. Rebouças*, Cláudio G. M. Filho*, Antônio B. S. Júnior*, Laurinda L. N. dos Reis*, Fabrício G. Nogueira*, Tobias R. F. Neto*, Luiz H. Barreto*, Bismark C. Torrico*

*Electrical Engineering Department
Federal University of Ceará
Fortaleza, Ceará, Brasil

Emails: lucas@dee.ufc.br, claudio@dee.ufc.br, barbosa@dee.ufc.br, laurinda@dee.ufc.br, fnogueira@dee.ufc.br, tobias@dee.ufc.br, lbarreto@dee.ufc.br, bismark@dee.ufc.br

Abstract— This work is a study and implementation of a Field Oriented Control (FOC) strategy using a Generalized Predictive Control (GPC) technique applied to the mechanic speed loop like as previous setting position controller. Thus aiming to obtain a system that acts in the small motor driver in low speed. The speed loop was identified to use as model to design the GPC controller. Experimental results are presented and discussed to demonstrate the importance of the proposed approach and also applying for the speed loop control to verify their behavior to such employment.

Keywords— AC motor, system identification, predictive control, variable speed drives

Resumo— Este trabalho é um estudo e implementação de uma estratégia de Controle de Campo Orientado utilizando a técnica de Controle Preditivo Generalizado aplicado à malha mecânica de velocidade de um motor de indução como controlador de posição. Assim, visando obter um sistema que atue em um motor de baixa potência e em baixas velocidades. A malha de velocidade foi identificada para ser usada como modelo para projetar o controlador preditivo generalizado. Resultados experimentais são apresentados e discutidos para demonstrar a importância da abordagem proposta.

Palavras-chave— Motores AC, identificação de sistemas, controle preditivo, motor de velocidade variável

1 Introduction

Induction machines (IM) are widely used in industry due to its simplicity, lower cost, reduced need for maintenance, and also due to its greater robustness if compared to other types of electrical machines. Usually, when necessary low speed is performed by employing DC motors. In the last two decades, advances have occurred in the study of principles that govern Field Oriented Control (FOC) applied to alternating current (AC) machines. Therefore, the control of induction machines can achieve performances similar to DC motors. In this type of control, a direct analogy can be established with the control of a DC motor with separate excitation (Bose, 2001).

There are several techniques for speed control applied to IM drives, the use of predictive strategies is one of them. The predictive model was employed in (Santana et al., 2008) to control both the speed and rotor flux. Additionally, (Beerten et al., 2010) uses a predictive strategy applied to the direct torque control (DTC) to decrease flux and torque ripple. Technical adaptations are widely used in (Jacobina et al., 2003), which uses the strategy named Model Reference Adaptive Control (MRAC) to control speed in the IM. Besides those studies, there are robust techniques of DTC to speed sensorless adjust using a predictive controller in a PI structure (Markadeh and Soltani, 2006).

In order to control the IMs, considering that speed is almost zero, a proper strategy is necessary. Studies regarding this subject are rarely found in literature. Previous works that have presented several studies have been developed in the control strategies for the MIT drive as (Souza et al., 2014), (Souza et al., 2015) and (Silva et al., 2015).

Therefore, this paper proposes the design of controller that acts on the speed loop in the Induction Motor. Substituting loop speed control traditional by the GPC control strategy using RST polynomial structure of control (Ljung, 1999).

The technology contribution of this study lies in the possible applications to robotics. When induction motors (IMs) are used, inexpensive, rugged, and easy to maintain units can be used in the joint degrees of freedom of the robot arm, for example. The main scientific contribution consists in the study GPC applied to speed control of IM. The use of the aforementioned control techniques GPC is justified by simplicity and ease of implementation in an embedded system. For instance, a DSC (Digital Signal Controller) is used in the proposed approach.

Finally, this work presents simulations tests and experimental results in order to demonstrate the main features of the developed system, thus validating the employed methodology. The paper is organized as follows. Section 2 and section 3 describes the induction motor modeling and the controller design, respectively. Section 4 presents the discussion of both simulation and experimen-

tal results, respectively. Finally, the proper conclusions are given in section 5.

2 Dynamic modeling of the indirect field-oriented control of an induction machine

The FOC block diagram is shown in Figure 1. The voltage source inverter (VSI), the space vector modulator and the control block with the position reference compose the system configuration. The SVPWM modulator converts the current control signals in the specifics switching functions for the VSI. The motor currents and the shaft position are used in its respective feedback loop.

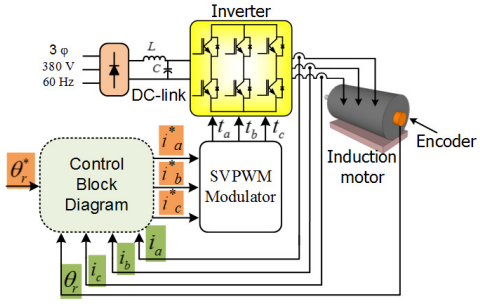

Figure 1: The field-oriented induction motor drive with the position control loop

The state-space model of the induction motor in the rotating dq- reference frame are given as follows (Bose, 2001):

$$\dot{\boldsymbol{x}} = \boldsymbol{Ax} + \boldsymbol{Bu} \tag{1}$$

Where:

$$\dot{x} = \begin{bmatrix} i_{ds} \\ i_{qs} \\ \lambda_{dr} \\ \lambda_{qr} \end{bmatrix}; \mathbf{B} = \frac{1}{\sigma L_s} \begin{bmatrix} \nu_{ds} \\ \nu_{qs} \\ 0 \\ 0 \end{bmatrix};$$

$$\mathbf{A} = \begin{bmatrix} -\frac{R_s}{\sigma L_s} - \frac{R_r(1-\sigma)}{\sigma L_r} & \omega_e & \frac{L_m R_r}{\sigma L_s {L_r}^2} & \frac{P\omega_r L_m}{2\sigma L_s {L_r}^2} \\ \omega_e & -\frac{R_s}{\sigma L_s} - \frac{R_r(1-\sigma)}{\sigma L_r} & \frac{-P\omega_r L_m}{2\sigma L_s {L_r}^2} & \frac{L_m R_r}{\sigma L_s {L_r}^2} \\ \frac{L_m R_r}{L_r} & 0 & -\frac{R_r}{L_r} & \omega_e - \frac{P}{2}\omega_r \\ 0 & \frac{L_m R_r}{L_r} & -(\omega_e - \frac{P}{2}\omega_r) & -\frac{R_r}{L_r} \end{bmatrix}$$

The electromagnetic torque T_e is given by:

$$T_e = \frac{3P}{4}\frac{L_m}{L_r}(i_{qs}\lambda_{dr} - i_{ds}\lambda_{qr}) \tag{2}$$

While expressions (3), (4), (5) give the following parameters:

$$\sigma = 1 - \frac{L_m^2}{L_s L_r} \tag{3}$$

$$\lambda_{qr} = L_m i_{qs} + L_r i_{dr} \tag{4}$$

$$\lambda_{dr} = L_m i_{ds} + L_r i_{qr} \tag{5}$$

In the field-oriented technique, the rotor flux linkage λ_r is assumed to be always aligned with the d-axis. Thus, the rotor flux linkage and its derivative in the q-axis is zero. Then, from (1) the d- and q- stator voltage equations are given in equations (6) and (7):

$$\sigma_{qs} = (R_s + (L_s - \frac{L_m^2}{L_r})s)i_{qs} + \omega_e L_s i_{ds} \tag{6}$$

$$\sigma_{ds} = R_s i_{ds} - \omega_e(-L_s - \frac{L_m^2}{L_r})i_{qs} \tag{7}$$

The rotor flux linkage can be found from (1) and assuming that the magnetizing stator current i^*_{ds} will be kept constant, it is possible to obtain:

$$\lambda_{dr} = L_M i_{ds} \tag{8}$$

Then, rewriting (2) the electromagnetic torque is given by:

$$T_e = \frac{3P}{4}\frac{L_m^2}{L_r} i^*_{qs} i^*_{ds} \tag{9}$$

The variable i^*_{qs} represents the torque current command generated from the speed controller and the variable i^*_{ds} remains constant because of the fixed value of the rotor flux linkage in (8).

The slip angular speed ω_{sl} is necessary to calculate the rotor flux linkage angular position θ_e in the indirect FOC theory. Thus, with the equations (4) and (1), the slip angular speed is obtained:

$$\omega_{sl} = \frac{L_m R_r i^*_{qs}}{L_r \lambda_{dr}} = \frac{R_r i^*_{qs}}{L_r i^*_{ds}} \tag{10}$$

With the value of the slip angular speed and shaft position θ_r given by the encoder, it is possible to obtain the rotor flux linkage angular position:

$$\theta_e = \theta_r + \underbrace{\int \frac{R_r i^*_{qs}}{L_r i^*_{ds}} dt}_{\theta_{sl}} \tag{11}$$

The equation (11) proves the indirect field-oriented control. In other words, it is possible to obtain the position of the rotor flux linkage indirectly through the position of the machine shaft and the slip angle between the stator and rotor magnetics fields.

3 GPC approach to model predictive control

The predictive control strategy requires a system model under study in order to compute the prediction inside the control horizons to be used. So

it is needed a preliminary study in order to find the model that best suit the system. Thereby, the predictive controller can be implemented. This section is subdivided into two subsections, one relating to the system modeling and another to the predictive control used.

3.1 System Modeling

There are various types of methodologies that can be used in the model system identification. For this process represented in Figure 1, the structure of the FOC scheme has been changed and presented in Figure 2. It was performed some steps in torque reference system being analyzed the output of rotor speed. This behavior can be observed in Figure 3. This data was used to identify the model, where half of the data was used for the identification process and the other half used for validation.

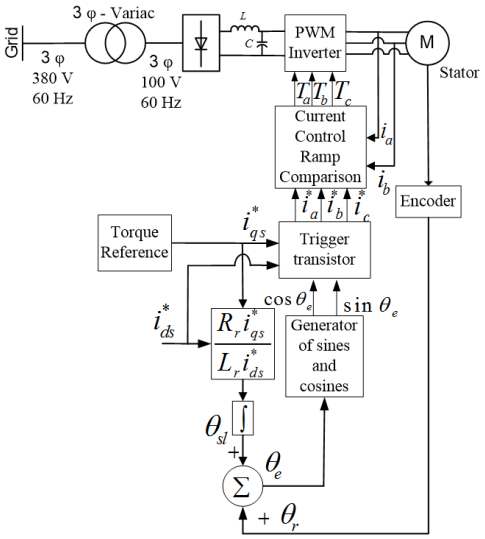

Figure 2: Structure used for identification

The process dynamics can be represented using the Controlled Auto-Regressive and Integrated Moving Average (CARIMA) model (Ljung, 1999) (Clarke et al., 1987):

$$A(q^{-1})y(t) = B(q^{-1})u(t) + \frac{C(q^{-1})}{\Delta}e(t), \quad (12)$$

where $e(t)$ is uncorrelated (white) noise with zero mean value, $A(q^{-1})$, $B(q^{-1})$ and $C(q^{-1})$ are polynomials in the backward shift operator q^{-1} in the form and $\Delta = 1 - q^{-1}$:

$$A(q^{-1}) = 1 + a_1 q^{-1} + a_2 q^{-2} + ... + a_{na} q^{-na},$$
$$B(q^{-1}) = b_0 + b_1 q^{-1} + b_2 q^{-2} + ... + b_{nb} q^{-nb},$$
$$C(q^{-1}) = 1 + c_1 q^{-1} + c_2 q^{-2} + ... + c_{nc} q^{-nc}.$$

From the data obtained in Figure 3, the least squares method was used (Ljung, 1999), and considering (12), the following discrete transfer function relating rotor speed output and reference torque, using 0.1 ms as sample time, is obtained by:

$$G(q^{-1}) = \frac{B(q^{-1})}{A(q^{-1})} = \frac{28.72}{1 - q^{-1}} \quad (13)$$

The polynomial $C(q^{-1})$ corresponds the model noise dynamics is modeled by a filter described in (Silva et al., 2015).

As the proposed controller is in the loop position, so just add an integrator in the system model.

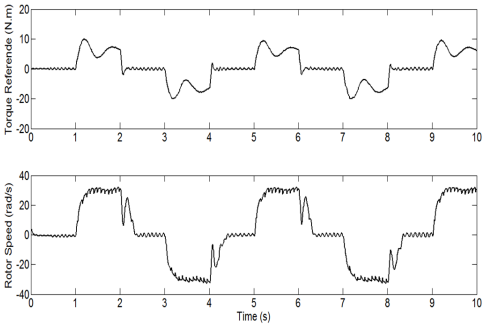

Figure 3: Input and output for system identification

3.2 Generalized Predictive Control

The GPC algorithm consists in applying a control sequence that minimizes a multistage cost function of the form (Clarke et al., 1987):

$$J = \sum_{j=N_1}^{N_2} [y(t+j \mid t) - \omega(t+j)]^2 + \sum_{j=0}^{N_u - 1} \lambda[\Delta u(t+j \mid 1]^2 \quad (14)$$

where N_1 and N_2 are the minimum and maximum costing horizons, respectively, N_u is the control horizon, λ is the control weight, $\omega(t+j)$ is a future setpoint or reference sequence, $\Delta u(t)$ is the incremental control action and $y(t+j \mid t)$ is the optimum j-step ahead prediction of the system output $y(t)$ on data up to time t.

The solution of this optimization problem is a crucial step in MPC (Model Based Control) algorithms. The numerical complexity depends on the characteristics of the models in terms of linearity, constraints, number of manipulated and controlled variables, etc. For linear models without constraints, the MPC optimization can be performed analytically (Camacho and Bordons, 2004).

The future outputs can be computed by using filtering techniques or Diophantine equations while this work uses the second approach. To compute the future outputs $y(t+j)$ for $j = N_1, \ldots, N_2$, the following Diophantine equation must be solved:

$$C(q^{-1}) = E_j(q^{-1})\Delta A(q^{-1}) + q^{-1}F_j(q^{-1}) \quad (15)$$

where $E_j(q^{-1})$ and $F_j(q^{-1})$ are uniquely defined polynomials with degrees $j-1$ and n_a, respectively.

Using (12) and (14) the future process output can be described by:

$$\begin{aligned} y(t+j) = \frac{F_j(q^{-1})}{C(q^{-1})}y(t) \\ +\frac{E_j(q^{-1})B(q^{-1})}{C(q^{-1})}\Delta u(t+j-1) \\ +E_j(q^{-1})e(t+j). \end{aligned} \quad (16)$$

As the degree of $E_j(q^{-1})$ is $j-1$, then all the noise terms are in the future, and therefore the optimal prediction can be obtained replacing $e(t+j)$ for its expected value (zero) as:

$$\begin{aligned} y(t+j \mid t) = \frac{F_j(q^{-1})}{C(q^{-1})}y(t) \\ +\frac{E_j(q^{-1})B(q^{-1})}{C(q^{-1})}\Delta u(t+j-1 \mid t). \end{aligned} \quad (17)$$

From (17), the past control inputs can be separated solving a new Diophantine equation:

$$E_j(q^{-1})B_j(q^{-1}) = H_j(q^{-1})C(q^{-1}) + q^{-j}I_j(q^{-1}), \quad (18)$$

where $H_j(q^{-1})$ has degree $j-1$ and $I_j(q^{-1})$ has degree $n_i = \max(n_a, n_b - j - 1)$. By using (17) and (18) the prediction output can be written as

$$\begin{aligned} y(t+j \mid t) = \frac{F_j(q^{-1})}{C(q^{-1})}y(t) \\ +\frac{I_j(q^{-1})}{C(q^{-1})}\Delta u(t+j-1) \\ +H_j(q^{-1})\Delta u(t+j-1 \mid t), \end{aligned} \quad (19)$$

which can be expressed in a vector form as:

$$y = F_j(q^{-1})\frac{y(t)}{C(q^{-1})} + I(q^{-1})\frac{\Delta u(t-1)}{C(q^{-1})} + G\Delta u, \quad (20)$$

where $y = [y(t+N_1 \mid t)y(t+N_1+1 \mid t)\dots y(t+N_2 \mid t)]^T$, $\Delta u = [\Delta u(t \mid t)u(t+1 \mid t)\dots u(t+N_u-1 \mid t]^T$, $\mathbf{G}$ is a N x N_u constant matrix based on the coefficients of $H_j(q^{-1})$, while $F(q^{-1})$ and $I(q^{-1})$ are polynomial vectors.

From controller implementation standpoint, an analytical solution with low computational cost is important. Thus, this work is concerned with the investigation of a special case where $N_u = 1$, $N_1 = 1$, $N_2 = N$ and $\lambda = 0$, then the optimal input is:

$$\Delta u(t) = (G^T G)^{-1}G^T(w - f) = k(w - f), \quad (21)$$

Where $\mathbf{k}$ is a constant vector with dimension 1 x N, $\mathbf{w}$ is a vector which contains the future reference and free response given by:

$$f = F(q^{-1})\frac{y(t)}{C(q^{-1})} + I(q^{-1})\frac{\Delta u(t-1)}{C(q^{-1})}, \quad (22)$$

Since Nu = 1, it is important to notice that the constrained controller is equivalent to clipping, a case valid only for monovariable systems. The term clipping assumes that the predictive controller does not take into account constraints while computing the optimal input, but only afterwards, performing hard limitations if constraints are violated.

Through some manipulations, (21) can be written in the RST form:

$$u(t) = \frac{1}{\Delta R(q^{-1})}(T(q^{-1})r(t) - S(q^{-1})y(t)), \quad (23)$$

where $r(t) = w(t+j)$ is the setpoint, $T(q^{-1}) = C(q^{-1})\Sigma_{i=1}^{N}k(i)S(q^{-1}) = \Sigma_{i=1}^{N}k(i)F_i(q^{-1})$, $R(q^{-1}) = C(q^{-1}) + q^{-1}\Sigma_{i=1}^{N}k(i)I_i(q^{-1})$. The RST structure is important from control analysis standpoint because it can be derived properties such as stability and robustness, as presented in (Silva et al., 2015).

And, considering the control polynomials R,S, and T are given by (Silva et al., 2015):

$$T(q^{-1}) = t_0 + t_1q^{-1} + t_2q^{-2}, \quad (24)$$

$$R(q^{-1}) = 1 + r_1q^{-1} + r_2q^{-2}, \quad (25)$$

$$S(q^{-1}) = s_0 + s_1q^{-1} + s_2q^{-2}. \quad (26)$$

4 Experimental Results

The structure proposed has been seen in Figure 4. For implement the GPC controller was used the user-specified parameters included in the proposed method that are $N_2 = 10$, $N_u = 1$.

By using (24) to (26) the parameters RST found were: $s_0 = -0.0861$, $s_1 = 0.1542$, $r_1 = -1.8939$, $r_2 = 0.8939$, $t_0 = 27.2541$, $t_1 = -51.7828$, $t_2 = 24.5968$.

For the experimental implementation of the system, a kit consisting of a DSC from *Texas Instruments*®® TMS320F2812 was used. The machine is a fractional horsepower three-phase squirrel cage IM, whose parameters are given in Table I.

The remaining instruments are Hall-effect current sensors, the auxiliary voltage sources,

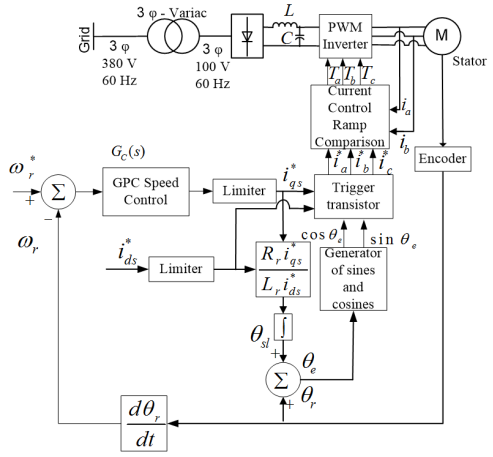

Figure 4: Control structure proposed using GPC strategy

Table 1: Motor Parameters

Parameters	**Value**
Rated power	0.25 HP
Rated speed	1725 rpm
Rated voltage	220 V
Rated currente	1.26 A
Number of poles	4
Rotor resistence (refered to the stator)	87.44 Ω
Stator resistence	35.58 Ω
Rotor inductance (refered to the stator)	0.16 H
Stator inductance	0.16 H
Mutual inductance	0.844 H
Inertial moment	$5 \ . \ 10^{-4} kg.m^2$
Viscous friction coefficient	$5.65 \ . \ 10^{-3} kg.m^2/s$

a three-phase voltage inverter module by *Semikron*® with a switching frequency of 2.5 kHz, a multi-turn precision potentiometer coupled to the motor shaft, with a sampling time of 0.4 ms and for the controller was used a sampling time of 10 ms for being a slow loop.

One DSC from *Texas Instruments*® TMS320F28335 carries out the controller. The three-phase squirrel cage IM has four poles, 0.25 HP and Y-connected windings. The specifications and parameters of the IM are given in Table I.

Figure 7 shows the behavior of the GPC control strategies proposed. By observing the tracking speed is very fast, around 0.1 seconds. Analyzing the behavior of the rotor speed steps no there oscillation after reaches reference and during changes reference are about 0 rad/s, 40 rad/s

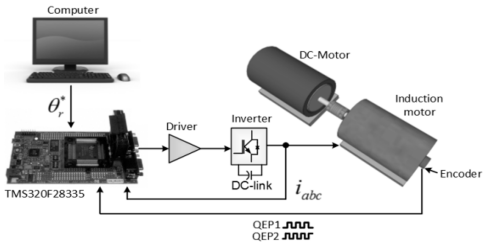

Figure 5: System's schematics

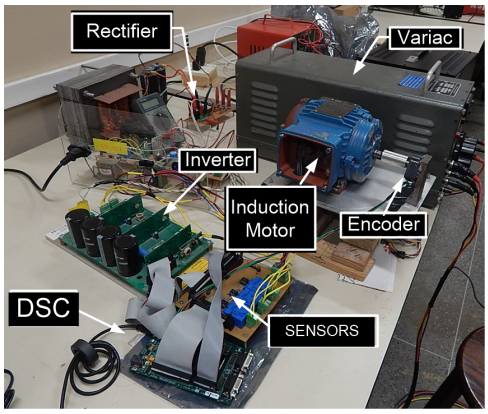

Figure 6: Experimental setup

and -40 rad/s. The currents i_d in the reference changes has peaks about 0.5 A and mean value about 0.3 A. And the i_q oscillates with peaks of 0.15 A and -0.15 A.

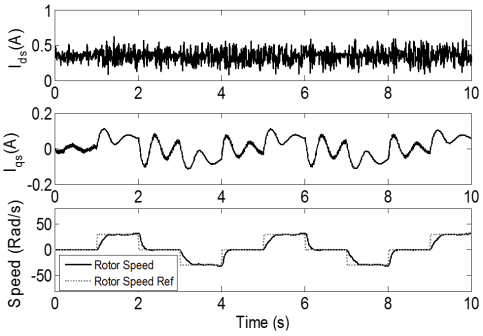

Figure 7: Experimental results for the system using GPC speed control strategy

After testing with the speed controller was implemented loop position control using a P-type controller. Obtaining the result shown in the Figure 8, showing the correct operation of the developed controllers. In the test performed were performed position steps from 2 radians to 6 radians with step 2 radians.

The schematics and one photo of the experimental setup are shown in Figures 5 and 6, respectively. The inverter is a 10 kVA industrial voltage-source three-phase inverter from *Semikron*®. The DSC produces a PWM switching frequency of 10 kHz and an incremental encoder, which is coupled to the motor shaft, gives the actual position. The

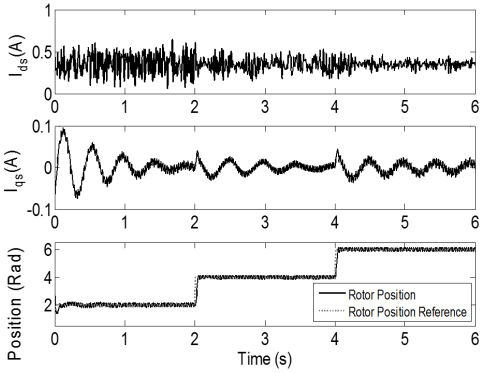

Figure 8: Experimental results for the position control using the GPC control proposed

DSC counter is used to count the encoder pulses and convert it to radians. The sampling time is 0.1 ms. The current sensors are Hall-effect current sensor from *LEM*®.

5 Conclusions

Controlling the low speed of an induction machine is particularly difficult due to existing inertia moments and low viscous friction coefficient, which brings complexity to the control. In order to analyze the performance of the controllers, the stator currents can be measured, thus representing the control system effort. The GPC strategy was then used in the studied plant providing the expected results, with good response to the reference and low swings in steady state. The use of a linear model simplifies the model structure and consequently the controller to be used. The purpose of this study is to use a relatively simple controller with the strength characteristics of the predictive strategy. In a previous work (Souza et al., 2015) it can be observed the use of classical models, where are shown that when PID was used, a longer time tracking position and a greater oscillation around the reference were achieved, as well as lower values of peak to i_{ds} and i_{qs}. Finally, such techniques can be applied to a robotic arm, while the actuation regarding of other motor and controller types are supposed to be investigated.

Acknowledgments

Special thanks to the DEE professors, as well as to CNPq for financial support. Project number 442573/2014-6.

References

Beerten, J., Verveckken, J. and Driesen, J. (2010). *Predictive direct torque control flux and torque ripple reduction*, IEEE Trans. Ind. Electron., vol. 57, n. 1, p. 404-412.

Bose, B. K. (2001). *AC machines for drives in Modern Power Electronics and AC Drives*, Prentice-Hall PTR.

Camacho, E. F. and Bordons, C. (2004). *Model Predictive Control*, Springer-Verlag.

Clarke, D. W., Mothadi, C. and Tuffs, P. S. (1987). *Generalized Predictive Control. Part I. The Basic Algorithm and Part II. Extensions and Interpretations*, Automática, vol. 23, n. 2, p. 137-16.

Jacobina, C. B., Ribeiro, L. A., Filho, J. B., Salvadori, F. and Lima, A. M. (2003). *Sistema de acionamento com motor de indução orientado indiretamente pelo campo com adaptação MRAC da velocidade*, Revista Controle e Automação, vol. 14, n. 1, p. 47-49.

Ljung, L. (1999). *System Identification - Theory for the User*, 2 edn, Prentice-Hall PTR.

Markadeh, G. R. A. and Soltani, J. (2006). *Robust direct torque and flux control of adjustable speed sensorless induction machine drive based on space vector modulation using a PI predictive controller*, Electr. Eng., vol. 88, n. 6, p. 485-496.

Santana, E. S., Bim, E. and Amaral, W. C. (2008). *A predictive algorithm for controlling speed and rotor flux of induction motor*, IEEE Trans. Ind. Electron., vol. 55, n. 12, p. 4398-4407.

Silva, W. A., Souza, A. B., Torrico, B. C., Honório, D. A., Neto, T. R. F., Reis, L. L. N. and Barreto, L. H. S. C. (2015). *Generalized predictive control robust for position control of induction motor using field-oriented control*, Electrical Engineering, vol. 97, n. 3, p. 195-204.

Souza, A. B., Diniz, E. C., Honório, D. A., Barreto, L. H. S. C. and Reis, L. L. N. (2014). *Hybrid control robust using logic fuzzy applied to the position loop for vector control to induction motors*, Electric Power Components and Systems, vol. 42, n. 6, p. 533-543.

Souza, A. B., Neto, T. R. F., Honorio, D. A., Diniz, E. C., Barreto, L. H. S. C. and Reis, L. L. N. (2015). *Hybrid position controller for an indirect field-oriented induction motor drive*, Eletrônica de Potência, vol. 19, n. 6, p. 343-353.